Structure *14*, 1179–1188, July 2006 DOI 10.1016/j.str.2006.05.019

Proteasome Assembly Triggers a Switch Required for Active-Site Maturation

Susanne Witt,[1,4] Young Do Kwon,[2,4,5] Michal Sharon,[3] Karin Felderer,[1] Mirjam Beuttler,[1] Carol V. Robinson,[3] Wolfgang Baumeister,[1,*] and Bing K. Jap[2,*]
[1] Department of Molecular Structural Biology
Max-Planck-Institute of Biochemistry
Martinsried, 82152
Germany
[2] Lawrence Berkeley National Laboratory
Berkeley, California 94720
[3] Cambridge University Chemistry Department
Cambridge, CB2 1EW
United Kingdom

Summary

The processing of propeptides and the maturation of 20S proteasomes require the association of β rings from two half proteasomes. We propose an assembly-dependent activation model in which interactions between helix (H3 and H4) residues of the opposing half proteasomes are prerequisite for appropriate positioning of the S2-S3 loop; such positioning enables correct coordination of the active-site residue needed for propeptide cleavage. Mutations of H3 or H4 residues that participate in the association of two half proteasomes inhibit activation and prevent, in nearly all cases, the formation of full proteasomes. In contrast, mutations affecting interactions with residues of the S2-S3 loop allow the assembly of full, but activity impacted, proteasomes. The crystal structure of the inactive H3 mutant, Phe145Ala, shows that the S2-S3 loop is displaced from the position observed in wild-type proteasomes. These data support the proposed assembly-dependent activation model in which the S2-S3 loop acts as an activation switch.

Introduction

The 26S proteasome (2.5 MDa) is the central enzyme of the ubiquitin pathway of protein degradation (Coux et al., 1996; Hershko and Ciechanover, 1998; Voges et al., 1999). This enzyme is comprised of the catalytic core complex (20S proteasome) sandwiched by two regulatory complexes, the 19S caps (Baumeister et al., 1998; Coux et al., 1996; Tanaka, 1998). The 20S proteasome occurs in all three kingdoms of life and is ubiquitous in archaea and eukaryotes, having a conserved overall architecture (Zwickl et al., 2000). Proteasomes have a barrel-shaped structure consisting of four stacked, seven-subunit rings that are arranged into two β rings sandwiched by outer α rings. Prokaryotic 20S complexes typically contain one α- and one β-type subunit, while eukaryotic proteasomes are formed with seven different α- and seven different β-type subunits (Zwickl et al., 1999). The proteolytic active centers of all proteasomes are located on the β subunits and situated in the central cavity of the proteasome barrel. Biochemical and genetic studies have shown that posttranslational processing of the β subunits, which removes the propeptides and activates the proteasome, is coupled directly to the assembly of the 20S proteasome in such a manner that active sites are formed after completion of the assembly (Zühl et al., 1997b). Therefore, activation of the 20S proteasome requires the docking and correct association of two half proteasomes to form a mature and fully active proteasome. The assembly of the full proteasome triggers the removal of the β subunit propeptide through autolysis at residue Thr1 that serves as the N-terminal nucleophile in substrate hydrolysis, leading to fully active enzymes (Seemüller et al., 1996). The precise orientation of the active site residue Thr1 is maintained by conserved residues, including those located on the S2-S3 loop. The highly regulated activation process requiring the assembly of full proteasomes provides a safeguard mechanism that prevents the occurrence of undesired protein degradation.

Knowledge of the molecular processes in proteasome assembly-dependent maturation is relatively limited. Point mutations in the β-trans-β (between two β rings) contact region perturb β-trans-β interactions and abolish proteolytic activity and, in many cases, proteasome assembly (Arendt and Hochstrasser, 1997; Chen and Hochstrasser, 1996). Chen and Hochstrasser (1996) have proposed that the active sites of the β subunits are formed upon the assembly of half proteasomes, involving interactions of helix H3 with its dyad related helix H3 of the β subunit on the opposing β ring. It was not clear, however, how the interactions of the helix H3 or the docking of two half proteasomes could trigger the formation of the active sites, which are some distance away from the contact region. Groll et al. (2003) reported that mutation of the active site residue could alter the nature of the contact regions between half proteasomes, including the structure and conformation of the S2-S3 loop.

Analysis of all structurally known proteasomes reveals that the association of half proteasomes involves interactions between residues on helix H4 of the β subunit, helix H3 of the dyad-related β subunit (β′ subunit), and the S2-S3 loop (Figure 1). In the 20S proteasome of *Rhodococcus erythropolis* (Kwon et al., 2004), helix H4 residues (Asp173 and Asp176) of the $\beta_{(1)}$ subunit form salt bridges with helix H3 residues (Lys152 and Lys151) on the dyad-related β subunit ($\beta'_{(1)}$ subunit) of the opposing ring. Helix H4 residues (Asp177 and Asp178) of the $\beta_{(1)}$ subunit also form a salt bridge and a hydrogen bond with the S2-S3 loop residues (Asn24 and Arg29) on the $\beta'_{(2)}$ subunit. Besides salt bridges and hydrogen bonds, hydrophobic interactions are found between helix H3 residues (Leu144 and Phe145) of one β subunit and the helix H3 residues (Phe145 and Leu144) of the opposing β subunit. The loop residues (Ile26 and Arg29) were found

*Correspondence: baumeist@biochem.mpg.de (W.B.); bkjap@lbl.gov (B.K.J.)
[4] These authors contributed equally to this work.
[5] Present address: Structural Biology Section, Vaccine Research Center, National Institutes of Health, Bethesda, Maryland 20892.

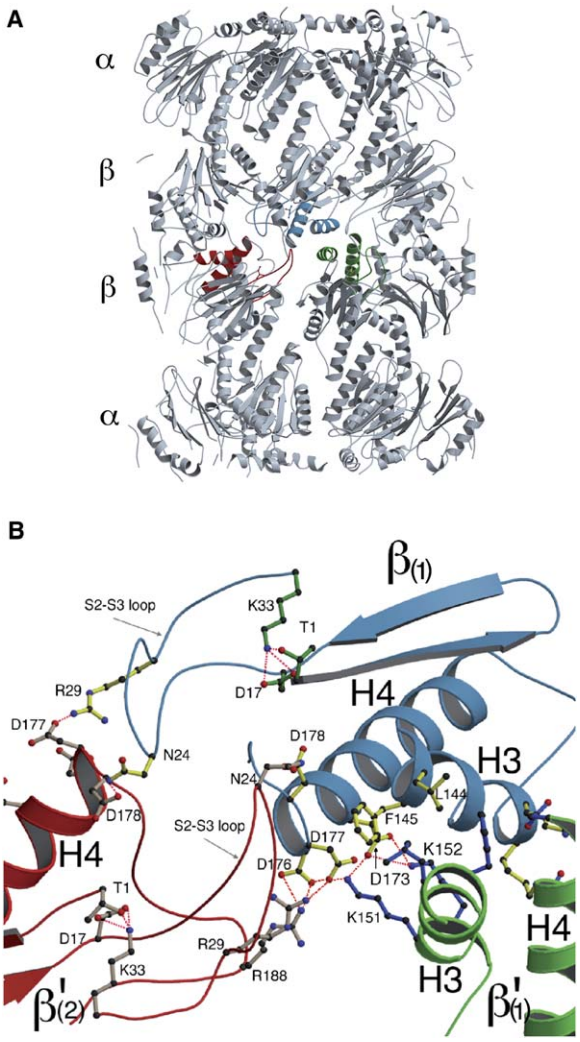

Figure 1. Ribbon Diagram of a Cut-Away Overview and Close-Up View of the 20S *Rhodococcus* Proteasome

(A) Cut-away view of the overall wild-type 20S *Rhodococcus* proteasome (PDB entry 1Q5Q) in ribbon presentation showing only three β subunits of the β-trans-β interface in which the respective helices H3 and H4 are highlighted in red, blue, and green.

(B) The magnified view of the color-highlighted β subunits. Residues involved in critical interactions are shown in ball-and-stick style, featuring residues involved in $\beta_{(1)}$-trans-$\beta'_{(1)}$ interactions between the helices H3 and H4 and those interactions between H4 of the $\beta_{(1)}$ and the S2-S3 loop of $\beta'_{(2)}$ of the opposing β ring. Loop residues Lys33 and Asp17 that coordinate active site residue Thr1 are also shown. The active site of the $\beta'_{(2)}$ is connected to the H4 helix of the opposing $\beta_{(1)}$ subunit through the S2-S3 loop. Disruption of the interactions between residues of the H4 helix with residues of the S2-S3 loop, such as through the dissociation of two half proteasome, can be expected to disturb the active site.

to form hydrogen bonds with the H4 backbone. Such interactions are so interrelated that perturbation of any of these salt bridges or hydrophobic residues is expected to affect the conformation of the S2-S3 loop. This loop contains residues necessary to form the substrate binding pocket and, more importantly, key residues, Asp17 and Lys33, required for the coordination of the active site residue, Thr1 (Figure 1B). These observations, together with earlier results provided by others, have led us to propose that salt bridges and hydrophobic interactions formed between two opposing half proteasomes, involving helices H3 and H4, drive the formation of full proteasomes that repositions the S2-S3 loops. Repositioning of this loop allows its conserved residues to correctly orient the active site residue, Thr1, leading to cleavage of the propeptide and activation of the proteasome.

To assess this model of proteasome maturation and activation, we studied *Rhodococcus* 20S proteasome mutants that contained mutations to residues of helices H3 and H4 that participate in the association of two half proteasomes and residues at the C-terminal loop of H4 that interact with residues of the S2-S3 loops of the opposing β ring. In addition, we report the crystal structure of the Phe145Ala (A) mutant of the *Rhodococcus* proteasome, along with mass spectrometry (MS) and biochemical analysis of a range of mutants. These results provide strong evidence in support of our assembly-dependent activation model.

Results and Discussion

To evaluate our assembly-dependent proteasome activation model, we performed biochemical and structural studies on proteasome mutants that were designed to disrupt β-trans-β (from two opposing half proteasomes) association. Based on our earlier crystal structure of the *Rhodococcus* proteasome (Kwon et al., 2004), we selected point mutants that were expected to alter hydrophobic and/or ionic interactions normally formed between two half proteasomes; this involved residues of the H3 and H4 helices and the residues of the C-terminal loop of the H4 helix that form contacts with the residues of the S2-S3 loop of the opposing β ring (Table 1). Mutants were expressed recombinantly in *E. coli* by using a bicistronic expression system, purified to homogeneity, and subjected to structural and biochemical analysis as well as mass-spectrometric examination. The proteolytic activities, assembly states, and active-site conformations were studied.

Biochemical Analysis of the β-Trans-β Interface Mutants

Both the wild-type and the mutant proteins were readily purified by a two-step purification scheme. After an affinity chromatography step targeting the C-terminal His-tags of the β subunits, the proteins were further purified on a Superdex 200 size-exclusion column to remove aggregates from correctly assembled proteasomes and half proteasomes. Biochemical analysis by native PAGE, SDS-PAGE, and size-exclusion chromatography (Figure 2) showed that the wild-type subunits assembled into 20S proteasomes with a size of approximately 750 kDa, corresponding to 14 α subunits and 14 processed β subunits.

In contrast to the wild-type proteasome, all but one of the β-trans-β interface mutants were found to be inactive with propeptides attached, indicating that the active site had been altered. One of the mutants (Asp177Ala) displayed a low level of activity. In native PAGE, mutants involving the substitution of residues of the helices H3 and H4 that participate in the association of the two opposing half proteasomes (KA [Lys151Ala-Lys152Ala], ADA [Phe145Ala-Asp173Ala-Asp176Ala], and AKA

Table 1. Overview of Alterations in the β-Trans-β Interface and the Relative Proteolytic Activity of the Respective Proteasome Mutants in Comparison to the Wild-Type

Name	Mutation	Disturbed Interaction	Phenotype	Relative Activity ± Rmsd (%)
WT	None	None	Fully assembled 28-mer (propeptides completely processed)	100 ± 1.23
A	Phe145Ala	Hydrophobic interaction H3-H3	Half proteasomes, with a modest fraction of full proteasomes (with partially degraded propeptides)[a]	0.67 ± 0.50
DA	Asp173Ala-Asp176Ala	Salt bridges from H4 to H3	Full proteasomes and a minor fraction of half proteasomes (with partially degraded propeptides)[a]	1.11 ± 0.57
KA	Lys151Ala-Lys152Ala	Salt bridges from H3 to H4	Half proteasomes (with partially degraded propeptides)[a]	1.30 ± 0.52
ADA	Phe145Ala-Asp173Ala-Asp176Ala	Hydrophobic interaction H3-H3; salt bridges from H4 to H3	Half proteasomes (with partially degraded propeptides)[a]	0.19 ± 0.62
AKA	Phe145Ala-Lys151Ala-Lys152Ala	Hydrophobic interaction H3-H3; salt bridges from H3 to H4	Half proteasomes (with partially degraded Propeptides)[a]	0.62 ± 0.65
D7	Asp177Ala	Salt bridge from the C-terminal loop of H4 to S2-S3 loop	Full proteasomes and a minor fraction of half proteasomes[a]	5.05 ± 0.66
D8	Asp178Ala	Salt bridge from the C-terminal loop of H4 to S2-S3 loop	Full proteasomes and a minor fraction of half proteasomes[a]	0.63 ± 0.62

[a] Compare to Figures 2 and 3.

[Phe145Ala-Lys151Ala-Lys152Ala]) appear exclusively as half proteasomes, while the A (Phe145Ala) and DA (Asp173Ala-Asp176Ala) mutants also contain a significant percentage of fully assembled proteasomes. However, in size-exclusion chromatography (Figure 2), the DA mutant shows a substantially different assembly distribution from that seen in native PAGE, showing an elution profile expected for wild-type proteasomes. This is likely the consequence of weakened interactions between half proteasomes due to the mutation. While this form of proteasome is stable in a size-exclusion column, the forces encountered due to the strong electric field in native PAGE were sufficient to dissociate the full proteasomes. Mutations involving changes of residues on the C-terminal loop of H4 (D7 [Asp177Ala] or D8 [Asp178Ala]) that interact with the residues Arg29 and Asn24 of the S2-S3 loop yield mostly full proteasomes as observed in both native PAGE and size-exclusion column chromatography (Figure 2). In contrast to the mutations that altered the interactions with the S2-S3 loop, the mutations disrupting the interactions between H3 and H4 helices have a destabilizing effect on full proteasome assembly, suggesting that the residues forming these critical interactions are likely to play the predominant role in half-proteasome association.

The requirement of correct proteasome assembly for activation is highlighted by the phenotype of the DA mutant that is seemingly not in line with those of other mutants involving substitution of residues of the helices H3 and H4. Based on the *Rhodococcus* wild-type proteasome structure, the DA mutant (Asp173Ala-Asp176Ala), which disrupts the interactions between Asp173/Asp176 and their counter residues Lys151/Lys152, could potentially form new salt bridges with Glu169/Asp177 residues located in the neighborhood of Asp173 and Asp176. These potential new interactions likely play a major role in the association of the two half proteasomes found in this mutant. This observation highlights the notion that activation requires not only the association of two half proteasomes but also correct alignment allowing for the appropriate repositioning of the S2-S3 loop for activation. This notion is consistent with the results of mutations of residues (Asp177Ala or Asp178Ala) on the C-terminal loop of H4 that interact with residues (Arg29, Asn24) of the S2-S3 loop that allow for the assembly of full, but activity impacted, proteasomes. The impact is seen in the form of complete inactivation (D8 mutant) or greatly reduced activity (D7 mutant). This result suggests that these two point mutations, while allowing for the formation of full proteasomes, still prevent the S2-S3 loops from being correctly repositioned for activation.

We investigated the relative stability of the wild-type proteasome and the half proteasome as well as the fully assembled proteasome mutants involving residues of helices H3 and H4 that participate in the interaction between two half proteasomes by either incubating the samples at room temperature for several weeks or flash freezing them in liquid nitrogen, followed by storage at −80ºC. After 14 days, the mobility of freshly frozen samples in native and SDS-PAGE was compared to that of the samples aged at room temperature (Figures 2A and 2B). The wild-type 20S proteasome is an extremely stable protein and is not altered by incubation at room temperature for several weeks. The various interface mutants exhibit differing aging behavior. Whereas the single point mutant A and the triple point mutants ADA and AKA are as stable as the wild-type and no change in assembly state or any accelerated subunit degradation can be detected, the DA and KA mutants as well as the D7 and D8 mutants change within the time course of several weeks. The double point mutants DA and KA are severely degraded after an incubation time of 4 weeks, resulting in a population of assembly states even smaller than half proteasomes.

We tested the proteolytic activity of the mutants by using a fluorescence-based activity assay and found that except for one, namely D7, they are all virtually inactive in comparison to the wild-type (Table 1). Proteolytic activities of the wild-type and the different mutants were compared by an assay that monitored the time-dependent increase in fluorescence caused by the release of the fluorescent dye during hydrolysis of the

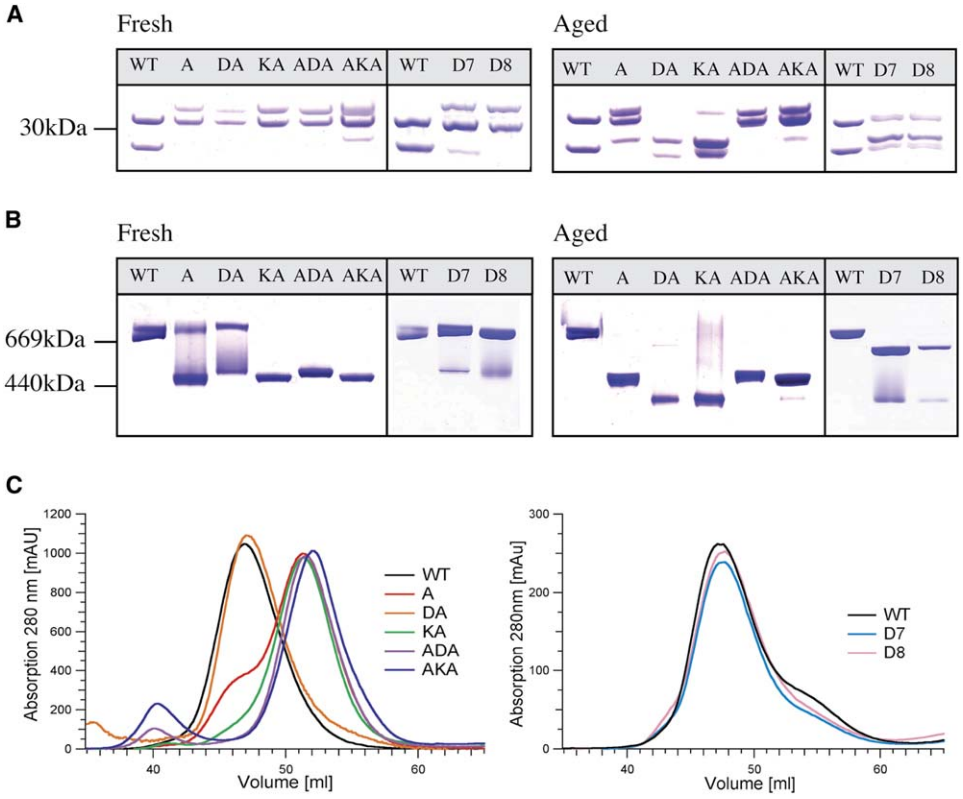

Figure 2. Biochemical Analysis of the Aging Process of the 20S Proteasome and Its Interface Mutants

(A and B) (A) Coomassie-blue-stained SDS-PAGE and (B) native PAGE analysis of the wild-type proteasome (wt) and the mutants A, DA, KA, ADA, AKA, D7, and D8. The notation "Fresh" refers to freshly purified protein. "Aged" stands for aged protein, which was incubated for 14 days at room temperature. As SDS marker, the "BenchMark Protein Ladder" for denaturing electrophoresis (Invitrogen) was used. The section between 20 and 40 kDa is shown. As native marker, the High Molecular Weight Calibration Kit for native electrophoresis (Amersham Biosciences) was used. In the shown section, this kit contains the following proteins: Thyroglobulin (669 kDa) and Ferritin (440 kDa).

(C) Size-exclusion chromatography of the wild-type proteasome (wt) and the two sets of mutants ([A, DA, KA, ADA, AKA] and [D7, D8]). These two sets were purified on two different Superdex 200 size-exclusion columns. The size-exclusion chromatogram of each set in comparison to the wild-type proteasome is shown individually.

Suc-Leu-Leu-Val-Tyr-AMC substrate. While the addition of substrate to the wild-type protein results in a steep increase of relative fluorescence continuing in a typical enzymatic saturation curve due to substrate exhaustion, the fluorescence of the substrate incubated with mutated proteins remained at a constant low value (Figure 3).

As indicated earlier, weakly assembled macromolecular complexes can be disrupted on native PAGE, or size-exclusion columns as has been shown for the 26S proteasomes (Udvardy, 1993; Yang et al., 2004). In order to visualize the assembly state of the β-trans-β interface mutants, electron micrographs of negatively stained proteasome samples were recorded (data not shown). Whereas the *Rhodococcus* wild-type exclusively shows the two characteristic views of the barrel-like structure, previously reported for these proteasomes (Mayr et al., 1998) and those of other species (Maupin-Furlow et al., 1998; Zwickl et al., 1992), all mutants, except for the double point mutant DA and the single point mutants D7 and D8, show mostly half proteasomes or other aberrant assemblies. In agreement with the biochemical data, the EM data support the hypothesis that the β-trans-β interactions mediated by the residues Phe145, Lys151, Lys152, Asp173, and Asp176 are crucial for full assembly that is required for active-site maturation.

Mass Spectra of the Wild-Type Proteasomes and the H3 and H4 Mutants

To examine the subunit composition of the different proteasome assemblies in more detail, nanoflow electrospray ionization mass spectrometry (ESI-MS) experiments were performed. The various proteasome mutants were introduced from solutions in which the native state of the complex is maintained, and spectra were recorded under MS conditions designed to preserve protein-protein interactions. The mass spectrum recorded for the wild-type 20S proteasome under these conditions is shown in Figure 4A. The charge state series centered at m/z ~11,000 is consistent with the mass calculated for 14 α subunits and 14 β subunits (743,866 Da). According to the mass determined for the wild-type proteasome (753,458 ± 154 Da), the β subunits do not contain remaining propeptides and are therefore fully processed. In the spectrum recorded for mutant A, the most intense charge states occur at lower m/z values (~8,500) and correspond to a species with molecular mass 423,630 ± 154 Da. This is consistent with assembly to the half-proteasome stage, and this species is predominant in the mass spectrum. At higher m/z values (~11,500) the signal is assigned to the full proteasome, although the charge states are not

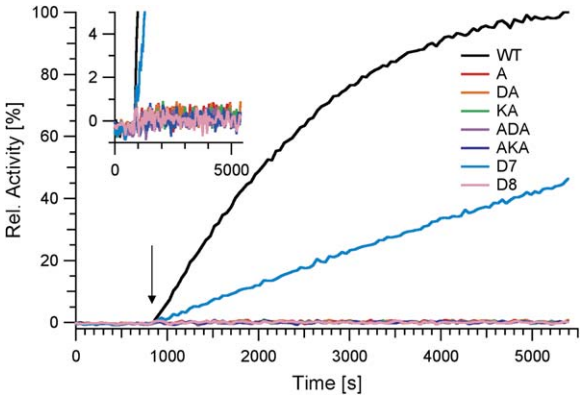

Figure 3. Relative Activity of the Mutants A, DA, KA, ADA, and AKA as Well as D7 and D8 in Comparison to the *Rhodococcus* 20S Wild-Type Proteasome

Proteolytic activity is assayed by the time-dependent relative increase in fluorescence caused by the release of the fluorescent dye during hydrolysis of the Suc-Leu-Leu-Val-Tyr-AMC. Equal amounts of protein (1 μg) in a total volume of 200 μl were incubated at 37ºC with a final concentration of 50 μM substrate. The fluorescence of Suc-Leu-Leu-Val-Tyr-AMC dissolved in buffer at the appropriate concentration represents the minimal value of fluorescence of the assay to occur. The black arrow indicates addition of the substrate. The inset represents an enlargement of the initial slope area.

resolved in this case. The spectra recorded for the DA mutant also shows a large fraction of full unprocessed proteasomes with a small fraction of half proteasomes, whereas the spectra recorded for the KA, ADA, and AKA mutants show only minor fractions of the full proteasome. The MS experiments are therefore in agreement with the results from the biochemical analysis and electron microscopy.

Tandem Mass Spectra of β-Trans-β Interface Mutants

To investigate the molecular composition of the individual subunits and their incorporation within the half proteasomes, we carried out tandem MS experiments in which an individual mass-to-charge state peak was isolated and subjected to collisional activation. This process results in the exclusion of a single protein subunit and the formation of a "stripped complex" (Aquilina et al., 2003). The tandem mass spectrum recorded for the ADA mutant is shown in Figure 4B. The 50+ charge state was isolated and activated to induce dissociation. Interestingly, only β subunits and not α subunits are observed in the resulting mass spectrum at low m/z. This is in contrast to the full proteasome where only α subunits are dissociated (Chernushevich and Thomson, 2004) and is consistent with their exposure in the fully assembled proteasome. For the half proteasome both α- and β subunits are exposed. The preferential dissociation of β subunits, however, is in accord with the known interactions in the *Rhodococcus* 20S proteasome (Kwon et al., 2004), where the contact area between two α subunits is almost twice that which exists between two β subunits. Therefore, this result reveals that the extent of interaction between protein subunits reflects the release of subunits in tandem MS of hetero-oligomeric complexes.

Expansion of the peaks assigned to the β subunits released during tandem MS reveals the modifications

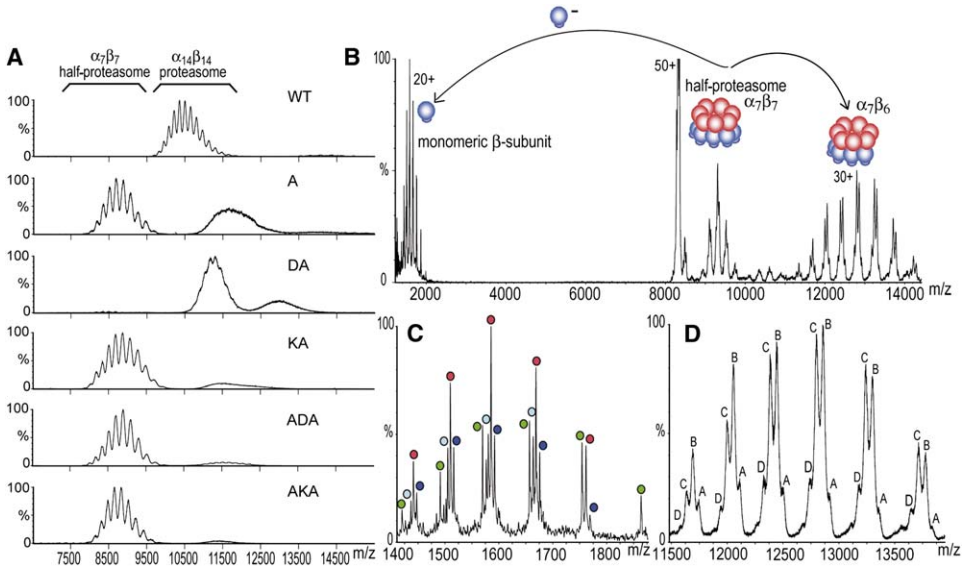

Figure 4. Mass Spectrometry of the Mutants A, DA, KA, ADA, AKA and Comparison with the Wild-Type Proteasome

(A) Nanoflow electrospray MS of the wild-type (wt) and mutants (A, DA, KA, ADA, AKA).

(B) The 50+ charge state of the ADA mutant was isolated for tandem mass spectrometry. The tandem mass spectrum confirms the stoichiometry of the half-proteasome species, composed of seven α subunits and seven β subunits, $\alpha_7\beta_7$. The dissociation process gives rise to individual β subunits at low m/z and stripped half-proteasome complexes at high m/z.

(C) This panel shows an expansion of the region of the spectrum assigned to monomeric β subunits dissociated from the complex. β subunits with the intact propeptide remaining are labeled with a blue circle. Red, light blue, and green circles denote propeptides in which the first methionine residue is absent (ΔM), the first two residues are removed (ΔMT), and the first 18 residues are cleaved (Δ18), respectively.

(D) This panel is an expansion of the stripped half-proteasome region assigned to $\alpha_7\beta_6$. The different species represent the incorporation of various truncated subunits. The subunit compositions are assigned as follows: A, $\alpha_7\beta_6'$; B, $\alpha_7\beta_5\beta^*$; C, $\alpha_7\beta_4\beta_2^*$; and D, $\alpha_7\beta_3\beta_3^*$; where β' and β* represent ΔMT and Δ18, respectively.

to the proteins. The measured masses of the modified forms confirm only partial degradation of the propeptides as opposed to complete degradation found in the wild-type proteasome. Moreover the peaks assigned to the "stripped complex," from which one β subunit has been dissociated (Figure 4D), reveal the incorporation of various truncated forms of the β subunit into the half proteasome assembly. Similarly tandem mass spectra recorded for the A, KA, and AKA mutants show that for both the fully assembled species as well as the half proteasomes, only partially degraded propeptides are present. Calculating the percentage of propeptide dissociation across the 1350–1900 m/z region reveals that only 18% of the β subunit propeptide remains intact, while for 37%, 20%, and 25% of the β subunits one, two, and eighteen, residues of the propeptides are cleaved, respectively. Interestingly, from the spectra recorded for all of the mutants examined in this study the extent of degradation of the propeptide was found to be closely similar between all of the mutants. This observation supports previous results, which show that the propeptides are degraded in a processive manner by undergoing multiple cleavages (Akopian et al., 1997; Mayr et al., 1998; Schmidtke et al., 1996).

Structural Analysis of the Phe145Ala Mutant

We have determined the crystal structure of the β subunit Phe145Ala mutant (A mutant) of the 20S proteasome from *Rhodococcus erythropolis* at 3.2 Å resolution. The packing of this mutant proteasome in the crystals was found to be similar to that of the wild-type proteasomes. As the biochemical, EM, and MS analysis indicated, there is a mixed population of half and full proteasomes in samples of this mutant; it appears that the crystallization process either selected for the subpopulation of full proteasomes and/or brought together half proteasomes through crystal-packing interactions. The overall structure of the mutant proteasome is nearly identical to that seen in the native wild-type (Kwon et al., 2004), except for relatively weak side chain electron densities for a number of α and β subunit residues: the side chains of α subunit residues (residue no. 10, 14, 18, 21, 22, 26, 28, 36, 44, 52, 56, 67, 92, 121, 126, 129, 130, 134, 161, 168, 169, 171, 172, 174, 177, 178, 186, 188, 189, 190, 203, 207, 217, 221, 235) and a larger number of β subunit residues (residue no. −44, −43, −35, −30, −28, −6, −5, −4, −3, −2, −1, 1, 3, 6, 9, 17–19, 22, 24, 25, 29, 32, 33, 39, 54, 112–116, 129, 147, 154, 157, 161, 165, 169, 171, 185, 188, 190, 199, 204, 207, 208, 212, 213, 215, 216) (Figure 5A). These residues were modeled as alanine. The overall quality of the data, indicated by the densities of the bulk of the map and reflected in the refinement statistics, supports the interpretation of weak side-chain densities as the result of high mobility. A summary of the refinement statistics is given in Table 2.

For the α subunit, the unmodeled residues were primarily located on the outer surface of the α ring; even in the higher-resolution wild-type structure, the corresponding residues were not very well defined (Figure 5B). For the mutant β subunits, regions neighboring the contact interface between two half proteasomes, specifically the helix H3, the helix H4, and the S2-S3 loop, show significant differences from those of the wild-type proteasome, where the backbone in these regions has a significantly higher B factor (Figure 5B). The high B factor of these regions resulted in densities of side chain residues, participating in the association of the two half proteasomes, too weak to be reliably modeled. This suggests that the improper assembly of the two half proteasomes destabilizes the structure around the contact regions. In addition, the backbones of the S2-S3 loops of the proteasome mutant are shifted away from the position observed in the wild-type proteasome by 1.4 Å (Figure 5C). The mutation also affects nearly all of the S2-S3 loop residues, including the key residues (Asp17 and Lys33) that directly support the orientation of the active site residue (Thr1). Many of the loop residues have very poor densities and cannot be confidently modeled. This includes the S2-S3 loop residues such as Asn24 and Arg29. In the wild-type structure, these two residues together with Ile25 are found to form hydrogen bonds with residues on the helix H4 of the opposing β subunit. The most striking differences between the wild-type and the Phe145Ala mutant structure are observed for three key residues, Thr1, Asp17, and Lys33. The side chains of these three residues are completely disordered in the mutant structure. Furthermore, the position of the Thr1 α carbon is shifted about 1.9 Å away from that of the wild-type proteasome.

Similar to the case of the Lys33Ala proteasome mutant (Kwon et al., 2004), most of the observable propeptide density is located in the antechambers; the propeptide residues Leu(−28) to Asn(−44) in both mutant structures are virtually identical. However, in contrast to the Lys33Ala mutant, residues Leu(−24) to Asn(−27) are not visible in the Phe145Ala mutant structure. In addition, while the six most C-terminal residues of the Lys33Ala propeptides, from Gly(−1) to Asp(−6) located in the central chamber region of the mutant structure, are clearly visible, only the α-carbon backbones of the corresponding residues are traceable in the Phe145Ala mutant structure.

The active-site region contains the propeptide residue Gly(−1), the active-site residue Thr1, and residues such as Asp17 and Lys33 located at the end of the S2-S3 loop. These residues are conserved throughout all active β subunits, and their conformations are known to be critical for propeptide removal (Ditzel et al., 1998). Mutation of any of these residues has been found to have drastic effects on propeptide processing (Chen and Hochstrasser, 1996; Schmidtke et al., 1996; Seemüller et al., 1996). The hydrogen-bond interactions found between Thr1 and two coordinating residues Asp17 and Lys33, involving Thr1Oγ, Asp17Oδ1, and Lys33Nε, are crucial for the precise positioning and orienting of the active-site residue and hence the activity of proteasomes (Figures 1B and 5C). Mutation of the active-site residue (Thr to Gly) has been reported to change regions of the structure, including what we refer to as the S2-S3 loop and the contact residues between two half proteasomes (Groll et al., 2003). Our biochemical data show that a single point mutation in 14 identical subunits, involving a relatively conservative substitution at the β-trans-β-interface, is sufficient to alter the interactions of the two half proteasomes. In the Phe145Ala mutant structure, it can be seen that this alteration results in displacing the S2-S3 loop away from its location in the wild-type

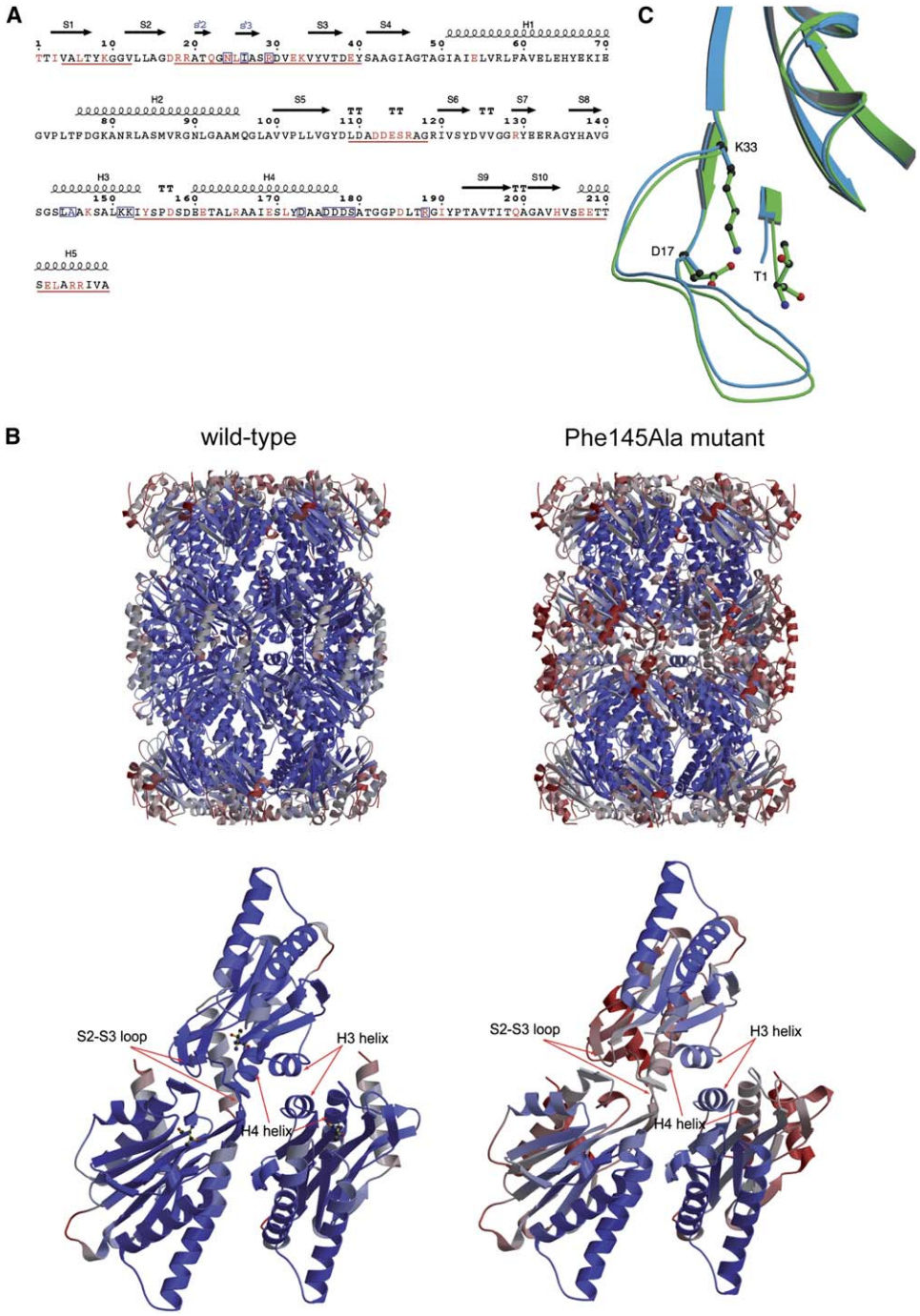

Figure 5. Mobility of the Overall Structure and Displacement of Active-Site Residues of the Phe145Ala Mutant in Comparison to the *Rhodococcus* Wild-Type

(A) The sequence and secondary structure of the Phe145Ala mutant *Rhodococcus* proteasome β subunit. The mutated residue is indicated by a blue letter. Residues whose side chains are disordered are shown in red letters, and residues that make β-trans-β contacts are blue boxed. Residues whose α-carbon B factor is higher than 80Å^2 are underlined in red. Following the nomenclature used in the *Thermoplasma* proteasome, helices are denoted as H1 to H5, and β sheets as S1 to S10. In the *Rhodococcus* structure, there are two small segments of β strands located within the S2-S3 loop, which are indicated as s′2 and s′3.

(B) Ribbon diagram of the wild-type proteasome and Phe145Ala mutant and the close-up view of the two β subunits and their trans β subunit of the opposing β ring, showing notably greater mobility of the mutant in regions at the β-trans-β interface. The α-carbon backbone regions with high B factors are shown in red and those with low B factors in blue. For clarity, the propeptides of the Phe145Ala mutant structure are not shown in the close-up view. In the close-up view of the wild-type structure, the active site residues (Thr1) are shown in ball-and-stick representation. The major differences of the α-carbon backbone are found at the S2-S3 loops and at the contact region.

(C) Superposition of the active-site regions of the wild-type (green) and the Phe145Ala mutant (blue) proteasomes in ribbon representation. Residues involved in formation of the wild-type active site, Thr1, Asp17, and Lys33 are shown in ball-and-stick representation; the equivalent residues in the mutant proteasome are disordered and therefore not shown or shown as Ala. The figure was produced with MOLSCRIPT and Raster3D.

Table 2. Summary of the X-Ray Crystallographic Data and Model Refinement Statistics of the Mutant Phe145Ala Proteasome

Data Collection	$(\alpha_1)_{14}(\beta_1[\text{Phe145Ala}]_{14})$
Space group	$C222_1$
Wavelength (Å)	1
Unit cell constants (Å)	
a	149.4
b	210.7
c	248.1
$\alpha = \beta = \gamma$	90°
Resolution (Å)	50–3.2 (3.60–3.45, 3.45–3.31, 3.31–3.20)
Completeness (%)	95.1 (96.3, 96.4, 95.1)
Number of total reflections	216,953
Number of unique reflections	61,090
Redundancy	3.6 (3.6, 3.5, 3.1)
R_{sym} (%)	9.0 (33.6, 48.3, 73.8)
I/δ	17.2 (3.7, 2.5, 1.3)
Refinement Statistics ($\|F\| > 0\ \delta$)	
Resolutions (Å)	20–3.2
$R_{cryst.}$ (%)	26.1
R_{free} (%)	28.8
Rmsd bonds (Å)	0.013
Rmsd angles (°)	1.6

Values in parentheses refer to the last three highest resolution shells. $R_{sym} = \Sigma|I - \langle I\rangle|/\Sigma\langle I\rangle$; I is the intensity of an individual measurement, and <I> its mean value. $R = \Sigma||F_o| - |F_c||/|F_o|$; F_o and F_c are observed and calculated structure factors, respectively. R_{free}; same as R but calculated for a subset of the reflections (10%), which were omitted during the refinement and used to monitor its convergence.

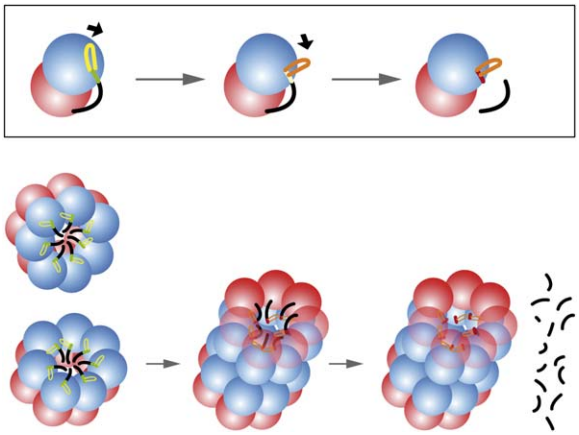

Figure 6. A Model of Assembly-Dependent Activation of Proteasomes

Prior to the association of the two half proteasomes (lower left), the S2-S3 loops are in an extended position as shown in the upper left of the top part of the figure. Upon association of the two half proteasomes (lower middle), the S2-S3 loops are repositioned. This repositioning of the loop, in turn, establishes the appropriate orientation of the active-site residues that supports the cleavage of the propeptides and activation of the proteasomes (lower right). The sequence of events is shown in close-up view in the top figures. Red spheres represent α subunits, and blue spheres depict β subunits with the S2-S3 loops shown in yellow prior to association of half proteasomes. The reorientation of the loop and the N-terminal active site region during assembly process are depicted by changes in their colors. The propeptides are shown in black line connected to the active site residue at the N-terminal end.

proteasome. Such a displacement alters S2-S3 loop residue interactions, some of which are critical for stabilizing the active-site residue, a condition necessary for the processing of the propeptide to occur. The importance of the correct positioning of the S2-S3 loop for the active site activation is further emphasized by the results of the mutants D7 and D8 described earlier.

In conclusion, our mutant structure and observations from biochemical studies of several mutants indicate that there is a strong coupling of the interaction at the interface of two half proteasomes and active-site formation, mediated by the S2-S3 loops. In this manner, the S2-S3 loop acts as an "activation switch" that couples proteasome assembly with the formation of the active site. The data presented here provide strong supporting evidence of our assembly-dependent activation model (Figure 6) that was developed based on earlier results from our lab and others. The model specifies that salt bridge and hydrophobic interactions, formed between two opposing half proteasomes involving 14 sets of helices (H3 and H4), provide the primary driving and aligning force for associating two half proteasomes that subsequently positions the S2-S3 loop "activation switches," allowing formation of the active sites and cleavage of the propeptides.

Experimental Procedures

Mutagenesis

The bicistronic expression plasmid pT7-7 β_1His_6-α_1 for the recombinant expression of the genes encoding the α_1 and the β_1 subunit, tagged with a C-terminal His_6-tag, of the 20S proteasome from *Rhodococcus erythropolis*, was a kind gift of Dr. Frank Zühl (Zühl et al., 1997a). This plasmid was used as a template for various site-directed mutagenesis experiments. Mutagenesis was performed with the QuikChange Site-Directed Mutagenesis Kit from Stratagene. The experiments were carried out according to the manufacturer's instructions. Several mutations in the β_1His_6-subunit were conducted, involving single-, double-, and triple-point mutations; these include Phe145Ala, Asp173Ala-Asp176Ala, Lys151Ala-Lys152Ala, Phe145Ala-Asp173Ala-Asp176Ala, and Phe145Ala-Lys151Ala-Lys152Ala, which are referred to as A, DA, KA, ADA, and AKA, respectively. Moreover, two single-point mutations, Asp177Ala and Asp178Ala, were conducted, which are referred to as D7 and D8, respectively (Table 1). The sequences of the mutant constructs were verified by nonradioactive DNA sequencing.

Expression and Purification

For expression, the *E. coli* strain BL21(DE3) (Stratagene) was transformed with the respective expression plasmid and grown in 6 l LB medium to mid-log phase at 37°C. After induction with a final concentration of 1 mM iso-propyl-β-D-thiogalactopyranoside (IPTG) for 5 hr, cells were harvested and resuspended in sonication buffer (20 mM Na-phosphate, 50 mM NaCl [pH 7.4]), treated for 30 min on ice with lysozyme (1 mg/ml, Sigma) and a few grains of DNaseI (Roche), and sonicated for 15 min (Sonifier 250, Branson). The lysate was further fractionated, first by a low-speed spin (4,500 × g, 15 min), followed by a high-speed spin (30,000 × g, 30 min). The supernatant was directly loaded onto a 5 ml His-trap column (GE Healthcare), previously equilibrated with buffer A (20 mM Na-phosphate, 500 mM NaCl, 20 mM imidazole [pH 7.4]). Nonspecifically bound protein was washed off with ten column volumes of buffer A. Proteasomes were eluted with a gradient of 20–500 mM imidazole. Fractions were analyzed by 12% Schaegger SDS-PAGE and 4%–12% Novex Tris-Glycine native PAGE (Invitrogen). Fractions containing 20S proteasomes were pooled, concentrated, dialyzed against gel filtration buffer (20 mM HEPES, 150 mM NaCl [pH 7.5]), and applied to a High Load 16/60 Superdex 200 (GE Healthcare) previously equilibrated with gel filtration buffer. Fractions were analyzed by 12% Schaegger SDS-PAGE and 4%–12% Novex Tris-Glycine native PAGE (Invitrogen). Fractions containing 20S proteasomes were

pooled and concentrated for subsequent crystallization trials and proteolytic activity assays.

Electrospray-Ionization Mass Spectrometry

Nanoelectrospray MS and tandem MS measurements were preformed on a QSTAR-XL modified for transmission of high-mass complexes (Sobott et al., 2002). This modified mass spectrometer has been fitted with a high-mass quadrupole capable of isolating ions up to 35,000 m/z (Chernushevich and Thomson, 2004). Prior to mass-spectrometry measurements, aliquots were buffer exchanged with Biorad Biospin columns into 1 M ammonium acetate solution and stored on ice. Typically, 2 μl of solution were electrosprayed from a gold-coated glass capillary prepared in house as described (Nettleton et al., 1998). The following experimental parameters were used (positive ion mode): capillary voltage up to 1.3 kV, declustering potential 150 V, focusing potential 250 V declustering potential 255 V, MCP 2350. In tandem MS experiments, the relevant m/z value was isolated, and argon gas was admitted to the collision cell with acceleration potential of up to 200 V. All spectra were calibrated externally by using a solution of cesium iodide (100 mg/ml). Spectra are shown here with minimal smoothing and without background subtraction.

Peptidase Assay

As a substrate, the synthetic fluorogenic peptide Suc-LLVY-AMC (Bachem, Heidelberg), dissolved in DMSO, was used. The determination of the kinetic parameters of Suc-LLVY-AMC hydrolysis was performed with the FluoStar Optima fluorescence spectrophotometer (BMG) at a reaction temperature of 37.0ºC ± 0.5ºC in 96-well format microtiter plates. After equilibration of 180 μl assay buffer (10 mM Tris-HCl, 100 mM NaCl [pH 7.5]) with 1.0 μg of purified wild-type or mutated enzyme (10 μl) for 10 min, in microtiter plates at 37ºC, 10 μl of 1 mM substrate solution (0.5% final concentration DMSO) was added, and fluorescence of the reaction mixture was measured immediately. Reaction progress was monitored at excitation and emission wavelengths of 320 and 460 nm, respectively, by measuring the relative fluorescence of each well every 30 s. Every experiment was repeated three to five times.

Crystallization

For crystallization purposes, concentration of the protein samples and buffer exchange was carried out with Amicon Ultra Centrifugal Filter Devices (100,000 MWCO). Crystallization trials were performed by the sitting-drop vapor diffusion method in VDX 24-well plates containing 1 ml of precipitant solution per well. In the crystallization wells, the protein, which was about 8 mg/ml in 10 mM Tris-HCl (pH 7.0) and 100 mM NaCl, was mixed with crystallization solution containing 16%–18% polyethylene glycol 3350, 50 mM sodium citrate at pH 7.5, in a 1 to 1 volume ratio. Single crystals of the mutant (Phe145Ala) grew in about 4 weeks and have average dimensions of 0.3 × 0.3 × 0.3 mm.

Data Collection and Structural Determination

The Phe145Ala mutant crystals were found to belong to orthorhombic space group $C222_1$ with cell dimensions a = 149.4 Å, b = 210.7 Å, and c = 248.1 Å. The raw X-ray data were indexed to 3.2 Å Bragg spacing and were scaled with HKL2000. For the initial phase calculation, molecular replacement was carried out with the coordinates of a half proteasome without propeptide ($\alpha_7\beta_7$) of the Lys33Ala mutant (PDB accession code 1Q5R) as a search model. The remaining steps of the structural determination and refinement were similar to those described in our work reported previously (Kwon et al., 2004). In our attempt to minimize introducing model bias for the initial phase calculation, we also used the $\alpha_7\beta_7$ model of the *Rhodococcus* wild-type proteasomes and that of the *Thermoplasma* as search models and obtained nearly identical results. The refinement converged to a crystallographic R factor of 0.261 (R_{free} = 0.288).

Acknowledgments

We would like to thank P.D. Adams and R.W. Grosse-Kunstleve for computational resources, N. To for help with crystallization, and beamline 8.3.1 staff of the Advanced Light Source for their assistance in data collection. M.S. acknowledges support from the European Molecular Biology Organization and from the Wingate Scholarship. S.W. would like to thank O. Dubiel for assistance.

Received: December 15, 2005
Revised: April 20, 2006
Accepted: May 2, 2006
Published: July 18, 2006

References

Akopian, T.N., Kisselev, A.F., and Goldberg, A.L. (1997). Processive degradation of proteins and other catalytic properties of the proteasome from *Thermoplasma acidophilum*. J. Biol. Chem. *272*, 1791–1798.

Aquilina, J.A., Benesch, J.L., Bateman, O.A., Slingsby, C., and Robinson, C.V. (2003). Polydispersity of a mammalian chaperone: mass spectrometry reveals the population of oligomers in alphaB-crystallin. Proc. Natl. Acad. Sci. USA *100*, 10611–10616.

Arendt, C.S., and Hochstrasser, M. (1997). Identification of the yeast 20S proteasome catalytic centers and subunit interactions required for active-site formation. Proc. Natl. Acad. Sci. USA *94*, 7156–7161.

Baumeister, W., Walz, J., Zühl, F., and Seemüller, E. (1998). The proteasome: paradigm of a self-compartmentalizing protease. Cell *92*, 367–380.

Chen, P., and Hochstrasser, M. (1996). Autocatalytic subunit processing couples active site formation in the 20S proteasome to completion of assembly. Cell *86*, 961–972.

Chernushevich, I.V., and Thomson, B.A. (2004). Collisional cooling of large ions in electrospray mass spectrometry. Anal. Chem. *76*, 1754–1760.

Coux, O., Tanaka, K., and Goldberg, A.L. (1996). Structure and functions of the 20S and 26S proteasomes. Annu. Rev. Biochem. *65*, 801–847.

Ditzel, L., Huber, R., Mann, K., Heinemeyer, W., Wolf, D.H., and Groll, M. (1998). Conformational constraints for protein self-cleavage in the proteasome. J. Mol. Biol. *279*, 1187–1191.

Groll, M., Brandstetter, H., Bartunik, H., Bourenkow, G., and Huber, R. (2003). Investigations on the maturation and regulation of archaebacterial proteasomes. J. Mol. Biol. *327*, 75–83.

Hershko, A., and Ciechanover, A. (1998). The ubiquitin system. Annu. Rev. Biochem. *67*, 425–479.

Kwon, Y.D., Nagy, I., Adams, P.D., Baumeister, W., and Jap, B.K. (2004). Crystal structures of the *Rhodococcus* proteasome with and without its pro-peptides: implications for the role of the propeptide in proteasome assembly. J. Mol. Biol. *335*, 233–245.

Maupin-Furlow, J.A., Aldrich, H.C., and Ferry, J.G. (1998). Biochemical characterization of the 20S Proteasome from the Methanoarchaeon *Methanosarcina thermophila*. J. Bacteriol. *180*, 1480–1487.

Mayr, J., Seemüller, E., Müller, S.A., Engel, A., and Baumeister, W. (1998). Late events in the assembly of 20S proteasomes. J. Struct. Biol. *124*, 179–188.

Nettleton, E.J., Sunde, M., Lai, Z., Kelly, J.W., Dobson, C.M., and Robinson, C.V. (1998). Protein subunit interactions and structural integrity of amyloidogenic transthyretins: evidence from electrospray mass spectrometry. J. Mol. Biol. *281*, 553–564.

Schmidtke, G., Kraft, R., Kostka, S., Henklein, P., Frommel, C., Lowe, J., Huber, R., Kloetzel, P.M., and Schmidt, M. (1996). Analysis of mammalian 20S proteasome biogenesis: the maturation of beta-subunits is an ordered two-step mechanism involving autocatalysis. EMBO J. *15*, 6887–6898.

Seemüller, E., Lupas, A., and Baumeister, W. (1996). Autocatalytic processing of the 20S proteasome. Nature *382*, 468–471.

Sobott, F., Hernandez, H., McCammon, M.G., Tito, M.A., and Robinson, C.V. (2002). A tandem mass spectrometer for improved transmission and analysis of large macromolecular assemblies. Anal. Chem. *74*, 1402–1407.

Tanaka, K. (1998). Molecular biology of the proteasome. Biochem. Biophys. Res. Commun. *247*, 537–541.

Udvardy, A. (1993). Purification and characterization of a multiprotein component of the *Drosophila* 26 S (1500 kDa) proteolytic complex. J. Biol. Chem. *268*, 9055–9062.

Voges, D., Zwickl, P., and Baumeister, W. (1999). The 26S proteasome: a molecular machine designed for controlled proteolysis. Annu. Rev. Biochem. *68*, 1015–1068.

Yang, P., Fu, H., Walker, J., Papa, C.M., Smalle, J., Ju, Y.M., and Vierstra, R.D. (2004). Purification of the *Arabidopsis* 26 S proteasome: biochemical and molecular analyses revealed the presence of multiple isoforms. J. Biol. Chem. *279*, 6401–6413.

Zühl, F., Seemüller, E., Golbik, R., and Baumeister, W. (1997a). Dissecting the assembly pathway of the 20S proteasome. FEBS Lett. *418*, 189–194.

Zühl, F., Tamura, T., Dolenc, I., Cejka, Z., Nagy, I., De Mot, R., and Baumeister, W. (1997b). Subunit topology of the *Rhodococcus* proteasome. FEBS Lett. *400*, 83–90.

Zwickl, P., Grziwa, A., Pühler, G., Dahlmann, B., Lottspeich, F., and Baumeister, W. (1992). Primary structure of the *Thermoplasma* proteasome and its implication for the structure, function, and evolution of the multicatalytic proteinase. Biochemistry *31*, 964–972.

Zwickl, P., Voges, D., and Baumeister, W. (1999). The proteasome: a macromolecular assembly designed for controlled proteolysis. Philos. Trans. R. Soc. Lond. B Biol. Sci. *354*, 1501–1511.

Zwickl, P., Baumeister, W., and Steven, A. (2000). Dis-assembly lines: the proteasome and related ATPase-assisted proteases. Curr. Opin. Struct. Biol. *10*, 242–250.

Accession Numbers

Atomic coordinates and structure factors (accession number: RCSB037991, PDB code: 2H6J) have been deposited in the Protein Data Bank, Research Collaboratory for Structural Bioinformatics, Rutgers University, New Brunswick, New Jersey (http://www.rcsb.org/).